Anisotropy in the Positron 2D Angular Correlation of Annihilation Radiation for Singly Negative Divacancies in Si

Z. Tang,[1] M. Hasegawa,[1] T. Chiba,[2] M. Saito,[3] A. Kawasuso,[1,*] Z. Q. Li,[1] R. T. Fu,[1] T. Akahane,[2] Y. Kawazoe,[1] and S. Yamaguchi[1]

[1]*Institute for Materials Research, Tohoku University, Sendai 980-77, Japan*

[2]*National Institute for Research in Inorganic Materials, Namiki 1-1, Tsukuba 305, Japan*

[3]*NEC Informatec Systems, Ltd., 34, Miyukigaoka, Tsukuba 305, Japan*

(Received 11 September 1996)

Interesting features of positron two-dimensional angular correlation of annihilation radiation (2D-ACAR) distribution for singly negative divacancies in Si are studied experimentally and theoretically. Anisotropy of the distribution is successfully detected for a specimen with aligned divacancies and is well reproduced by first-principles calculations based on the two-component density-functional theory. The present calculation demonstrates that the anisotropy reflects the characteristic distribution of electrons around the divacancies, indicating that the 2D-ACAR is an effective tool to provide microscopic information on vacancy-type defects. [S0031-9007(97)02701-4]

PACS numbers: 78.70.Bj, 71.55.Cn, 71.60.+z

The positron annihilation technique has recently emerged as a powerful tool to study vacancy-type defects in semiconductors. Positrons are sensitively trapped at defects and are annihilated with the surrounding electrons, conveying significant information on the local electronic environment around the defect site with the emitted two γ photons [1]. Especially the two-dimensional angular correlation of annihilation radiation (2D-ACAR) technique provides more detailed microscopic information about defects, compared with conventional techniques, e.g., measurement of positron lifetime or annihilation energy (Doppler broadening) spectrum [2–4]. The 2D-ACAR technique measures *two-dimensional* projection of the momentum distribution of the annihilated e^--e^+ pair (the integration of the three-dimensional momentum distribution over a chosen axis is observed) and has been used mainly for studies of electronic band structures of perfect crystals (bulk) [2]. Recently several groups have employed this method for studies of vacancies in semiconductors and have clarified that the distribution is significantly different in the annihilation site between bulk and vacancies: the momentum distribution for the bulk is quite anisotropic around the origin and those for vacancies are nearly isotropic [4–8]. Because of this difference, the 2D-ACAR technique is established as a sensitive probe of vacancy-type defects.

In spite of the above achievement, discussions on the relation between the observed momentum distribution and microscopic structures of defects are insufficient. Especially when the electron distribution around a defect is quite anisotropic, the observed momentum distribution should reflect this anisotropic nature and is thus expected to provide useful information on the local electronic environment around the defect. An interesting example discussed here is the Si divacancy, which is one of the fundamental stable defects existing at room temperature in Si and is crucially important in the Si technology [9]. Two adjacent Si atoms are removed in the divacancy with the six nearest Si atoms and the resulting electron distribution is quite different between the axis connecting the two vacancy sites ([111]) and the plane perpendicular to the axis.

In this Letter, we clarify that the above anisotropic electron distribution around the Si divacancy is successfully detected by the 2D-ACAR technique. In our recent attempt, the 2D-ACAR for divacancies in Si were found to be almost isotropic but weak anisotropy was detected when the divacancies were aligned by stressing the specimen at elevated temperature [7,8]. In this study, we present details of experimental results and clarify important features of the anisotropy. Moreover, the observed anisotropy is well reproduced by first-principles calculations based on the two-component density functional (TCDF) theory within the local density approximation (LDA) [10,11]. The used method was found from recent studies to be highly reliable for positron annihilation rates [11–13]. It is found from the present calculations that electrons in the dangling bonds of the nearest neighboring atoms make a significant contribution to the positron annihilation and the observed anisotropy originates from the characteristic distribution of these electrons. The present success, detection of the anisotropy and good agreement between experiment and theory, suggests that the 2D-ACAR technique is an effective tool to study microscopic structures of defects.

In the present experiment, the floating-zone-grown Si crystal doped with 1.0×10^{16} cm^{-3} phosphorus was irradiated with 15 MeV electrons to 5×10^{17} e/cm^2 at room temperature to obtain singly negative divacancy (V_2^{1-}) [14]. The divacancy V_2^{1-}, which has the four equivalent axes ([$11\bar{1}$], [$1\bar{1}1$], [$\bar{1}11$], and [111]) connecting the two-vacant sites, was aligned by the stressing treatment

 0031-9007/97/78(11)/2236(4)$10.00

after Watkins and Corbett [15]. We applied compressing uniaxial stress along the [011] axis to 500 kg/cm^2 at 170 °C for 1 hour and then cooled the specimen down to room temperature with stress on. An electron spin resonance (ESR) experiment [15] indicates that the above procedure increases the population (n_{in}) of the axes ([$1\bar{1}1$] and [$11\bar{1}$]) in the (011) plane and decreases that (n_{out}) for the out of plane ([$\bar{1}11$] and [111]). The degree of alignment ($n_{\text{in}}/n_{\text{out}}$) is estimated to be 1.2 based on results of the ESR study of the energy change due to switching the divacancy orientation [15]. The 2D-ACAR was then obtained using the machine of Anger camera type and the [001] (p_z) axis was chosen as the integration one. The observed 2D-ACAR includes the contributions from the annihilation both in the bulk and at divacancies. Since the divacancy component is quite different from the bulk component in their shapes, the divacancy component can be definitely decomposed from the observed "total" 2D-ACAR [7,8]. The decomposition was based on a least-square fitting to reproduce bulk anisotropy, which was obtained from a defect-free sample. The uncertainty of the procedure was estimated to be less than 2% in its intensity by the reproducibility of several measurements. The shapes of 2D-ACAR for the divacancy component obtained at 15, 100, 200, and 295 K are found to resemble each other. We therefore have summed up all the data at each temperature to have better statistics. The 2D-ACAR on the (001) plane for the *completely* aligned divacancies ($n_{\text{out}} = 0$) was then deduced from that for $n_{\text{in}}/n_{\text{out}} = 1.2$ [15]; hereafter we refer to this simply as the 2D-ACAR, unless otherwise stated. The details of the experimental setup were previously described [7,8].

The 2D-ACAR distribution obtained in the above experiment is found to have a definite anisotropy [Fig. 1(a)]. The distribution is slightly narrower along the [$01\bar{1}$] than along the [011] axis. We evaluate the full width at half maximum (FWHM) of the 2D-ACAR and find that FWHM on the p_x axis (8.8 mrad) is slightly smaller than that (9.0 mrad) on the p_y axis (Table I). We extract the anisotropic component $A(p_x, p_y)$ from the observed 2D-ACAR $N(p_x, p_y)$ as $A(p_x, p_y) = N(p_x, p_y) - C(p_x, p_y)$, where $C(p_x, p_y)$ is a smooth cylindrical average of $N(p_x, p_y)$ around the p_z axis [2,5,6] [Fig. 1(b)]. It was found that the values of $A(p_x, p_y)$ are negative on the p_x axis in sharp contrast with the positive values on the p_y axis [Fig. 1(b)]. A valley and a peak appear at 7 and 5 mrad on the p_x and p_y axes, respectively (Table I) [16]. It is emphasized that the above difference in the momentum density between the p_x and p_y axes was not observed when divacancies are randomly oriented ($n_{\text{in}} = n_{\text{out}}$). The difference thus originates from the fact that the divacancies are aligned in the (011) plane by the stress treatment: Because of this alignment, the [$01\bar{1}$] and [011] axes are inequivalent in the 2D-ACAR distribution. We then analyze the observed anisotropy in the 2D-ACAR based on the first-principles calculations in the following.

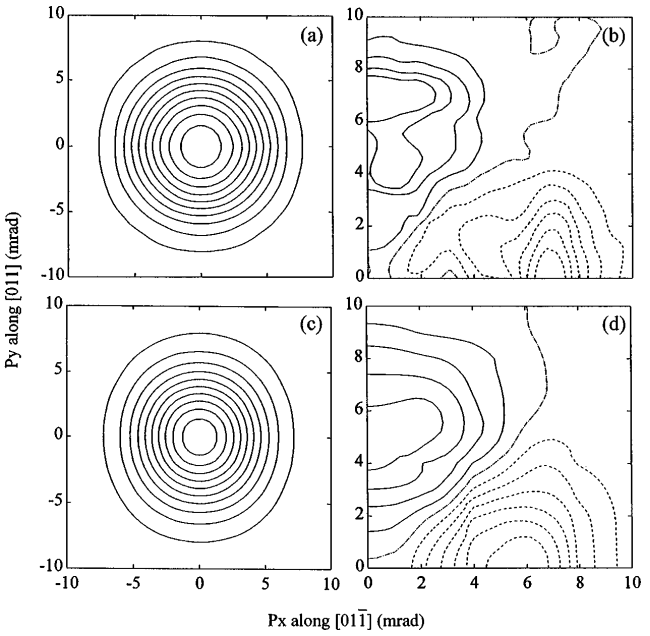

FIG. 1. (a),(c) Contour plots of trapped positron 2D-ACAR distribution $N(p_x, p_y)$ for aligned divacancies V_2^{1-} projected along the [100] direction: (a) experiment and (c) calculation. The contour spacing is one-tenth of the maximum value. Their anisotropies $A(p_x, p_y)$ are shown in (b) experiment and (d) calculation. The contour spacings in (b) and (d) are one-seventh of the absolute values of the valley; solid (dashed) lines indicate positive (negative) values.

The present calculations are based on the TCDF theory within the LDA [10,11]. We adopted the LDA scheme given by Puska et al. [11]: The electron-positron correlation energy was deduced from numerical results for homogeneous electron-positron plasmas [17]. The ion-electron and ion-positron interactions were represented by a nonlocal norm-conserving pseudopotential [18] and by a local potential [19], respectively, and the plane waves with the maximum kinetic energy of 210 eV were employed as the basis set. The 64-site supercell was used for describing the divacancy in the crystal and the Brillouin zone integration was performed using special k points [20] for the electrons [21] and the Γ point for the positron. All the atoms in the cell were relaxed in the geometry optimization in order to take medium range of relaxation. Minimization of the total energy over the

TABLE I. FWHM of the cross section of 2D-ACAR of the aligned V_2^{1-} and extremum positions in the anisotropy. In the experiment, the statistical errors are less than 1% for the FWHM and less than 5% for the extremal position.

	FWHM (mrad)		Extremum position in $A(p_x, p_y)$ (mrad)	
	Theory	Experiment	Theory	Experiment
p_x [$01\bar{1}$]	7.8	8.8	5.5	7
p_y [011]	8.2	9.0	5.4	5

degrees of freedom of positron and electron densities and atomic positions was performed using the conjugate-gradient iterative minimization technique [22,23]. After obtaining electron's and positron's wave functions (ψ_i^- and ψ^+) for the optimized geometry, we calculated the momentum density by

$$\rho(\mathbf{p}) = \text{const} \times \sum_i \left| \int e^{i\mathbf{pr}} \psi^+(\mathbf{r}) \psi_i^-(\mathbf{r}) \sqrt{g(\mathbf{r})}\, d\mathbf{r} \right|^2, \quad (1)$$

where the enhancement factor $g(\mathbf{r})$ is obtained based on the two-component plasma model and is thus consistent with the above electron-positron correlation energy [11]. Details of the method will be presented elsewhere.

We started with the determination of geometry of divacancy (V_2^{1-}) capturing a positron. In the symmetry conserving geometry optimization (D_{3d}) for V_2^{1-}, the nearest six atoms are displaced outwards (away from the vacancy site) by 0.06 Å. This outward displacement is in sharp contrast with the inward displacement when the vacancy does not capture the positron [24]. It is found for the optimized geometry that the highest occupied gap level (e_u) is doubly degenerate and is partially occupied by three electrons. The symmetry lowering (Jahn-Teller effect) from D_{3d} to C_{2h} is thus expected [15]. It is, however, found from the symmetry unrestricted calculation that the Jahn-Teller displacements of the nearest atoms are very small (less than 0.02 Å). We thus neglect the effect in the following calculation on the 2D-ACAR. A very small Jahn-Teller effect is expected to originate from the fact that the interaction between the dangling bonds is weak because of the outward displacements of the nearest atoms.

The 2D-ACAR for the aligned divacancy was calculated and the results are shown in Fig. 1 and Table I. The calculation is found to well reproduce significant features of the anisotropy observed in the present experiment: In the calculated 2D-ACAR, the FWHM on the p_x axis is slightly smaller than that on the p_y axis (Fig. 1 and Table I); the theoretical values of $A(p_x, p_y)$ are negative and positive along the p_x and p_y axes, respectively [Fig. 1(d)]; the positions of the extremum on the p_x and p_y axes are consistent with the experimental ones (Table I). Good qualitative agreement between experiment and theory is thus obtained. It is noted, however, that the theoretical 2D-ACAR distribution is slightly (about 10%) narrower than the experimental one as is indicated by FWHMs listed in Table I. Calculation beyond the LDA might thus be necessary for more quantitative discussion but is beyond the scope of this Letter.

We finally discuss the origin of the anisotropy in the 2D-ACAR based on the present numerical results. It is found that the positron is localized around the divacancy center, i.e., the middle point between the two vacancy sites [Fig. 2(a) and 2(b)]. As a result, the e^--e^+ pair distribution, represented by the product (overlap) of the

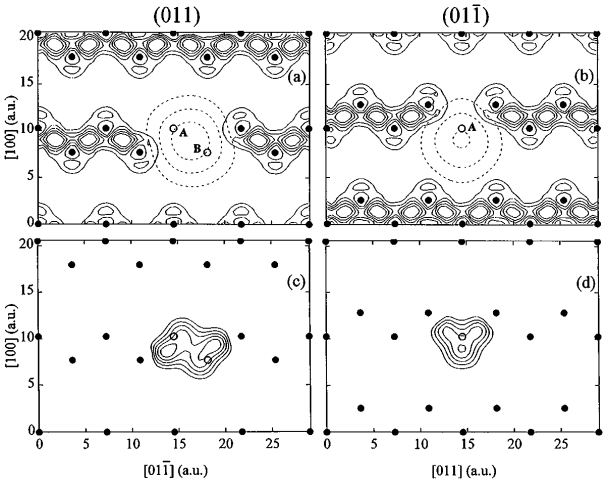

FIG. 2. The charge densities of the electrons and positrons associated with the aligned divacancies V_2^{1-} ([1$\bar{1}$1] axis) together with their overlap in the (011) and (01$\bar{1}$) planes: (a) charge densities of e^- (solid lines with the contour spacing of $1.0 \times 10^{-2} e^-/a_0^3$) and e^+ (dashed lines: 1.5, 15 and $75 \times 10^{-4} e^+/a_0^3$) in (011), (b) the densities in (01$\bar{1}$), (c) the density overlap in (011) with the contour spacing of 5.0×10^{-6} $(e^-/a_0^3)(e^+/a_0^3)$, and (d) the density overlap in (01$\bar{1}$). The two vacancies (A and B) of V_2^{1-} are denoted by the open circles, and the Si atoms are shown by the closed circles.

electron and positron densities [Figs. 2(c) and 2(d)], is localized in the dangling bond regions of the nearest six atoms. Since the distance between the nearest atoms on the zigzag chain in the [01$\bar{1}$] direction is large compared with that for the case of [011] direction, the e^--e^+ pair distribution is rather *broad* on the [01$\bar{1}$] axis as illustrated in Fig. 2. We expect that this characteristic e^--e^+ pair distribution in the real space is the origin of the observed anisotropy in the momentum space; the 2D-ACAR distribution on the p_x ([01$\bar{1}$]) axis is *narrower* than that on the p_y ([011]) axis as mentioned above.

In conclusion, 2D-ACAR for the divacancies with singly negative charge has been studied experimentally and theoretically. Interesting anisotropy is experimentally detected after stressing at 170 °C along the [011] axis. Characteristic features of the observed anisotropy are well reproduced by the calculations based on the TCDF theory within the LDA. It is found that the anisotropy originates from different electron-positron overlap densities along the two inequivalent axes ([011] and [01$\bar{1}$]) of the aligned divacancies. The present study demonstrates that the 2D-ACAR technique provides useful information on microscopic structures of vacancy-type defects in semiconductors.

The authors express sincere thanks to Professor M. Suezawa and Professor K. Sumino of Tohoku University for their invaluable suggestions and support for this work, and to the Information Science Group of the Institute for Materials Research, Tohoku University, for its continuous support for using the supercomputing system. They are

also grateful to Biosym Company for the special offer of the CASTEP program. This work is partly supported by a Grant-in-Aid for Scientific Research of the Ministry of Education, Science and Culture (No. 08650762), and by the Seki Memorial Foundation for Promoting Science and Technology.

*Present address: Japan Atomic Energy Research Institute, Takasaki Establishment, 1233 Watanuki, Takasaki 370-12, Japan.

[1] For example, see *Positron Spectroscopy of Solids*, edited by A. Dupasquier and A. P. Mills, Jr. (IOS Press, Amsterdam, 1995).

[2] A. A. Manuel, in *Positron Spectroscopy of Solids* (Ref. [1]), p. 155.

[3] P. Asoka-Kumar, K. G. Lynn, and D. O. Welth, J. Appl. Phys. **76**, 4935 (1994).

[4] S. Tanigawa, A. Uedono, L. Wei, and R. Suzuki, in *Positron Spectroscopy of Solids* (Ref. [1]), p. 729; S. Tanigawa, Hyperfine Interact. **79**, 575 (1993).

[5] R. Ambigapathy, A. A. Manuel, P. Hautojärvi, K. Saarinen, and C. Corbel, Phys. Rev. B **50**, 2188 (1994); R. Ambigapathy, C. Corbel, P. Hautojärvi, A. A. Manuel, and K. Saarinen, J. Phys. Condens. Matter **7**, L683 (1995).

[6] J. P. Peng, K. G. Lynn, M. T. Umlor, D. J. Keeble, and D. R. Harshman, Phys. Rev. B **50**, 11 247 (1994).

[7] T. Chiba, A. Kawasuso, M. Hasegawa, M. Suezawa, T. Akahane, and K. Sumino, Mater. Sci. Forum **175–178**, 327 (1995).

[8] M. Hasegawa, K. Kawasuso, T. Chiba, T. Akahane, M. Suezawa, S. Yamaguchi, and K. Sumino, Appl. Phys. A **61**, 65 (1995); M. Hasegawa, T. Chiba, A. Kawasuso, T. Akahane, M. Suezawa, S. Yamaguchi, and K. Sumino, Mater. Sci. Forum **196–201**, 1481 (1995).

[9] G. D. Watkins, in *Deep Centers in Semiconductors*, edited by S. T. Pantelides (Gordon and Breach, New York, 1986), p. 147.

[10] E. Boroński and R. M. Nieminen, Phys. Rev. B **34**, 3820 (1986); M. J. Puska and R. M. Nieminen, Rev. Mod. Phys. **66**, 841 (1994); R. M. Nieminen, in *Positron Spectroscopy of Solids* (Ref. [1]), p. 443.

[11] M. J. Puska, A. P. Seitsonen, and R. M. Nieminen, Phys. Rev. B **52**, 10 947 (1995).

[12] L. Gilgien, G. Galli, F. Gygi, and R. Car, Phys. Rev. Lett. **72**, 3214 (1994).

[13] M. Saito and A. Oshiyama, Phys. Rev. B **53**, 7810 (1996).

[14] A. Kawasuso, M. Hasegawa M. Suezawa, S. Yamaguchi, and K. Sumino, Jpn. J. Appl. Phys. **34**, 2197 (1995).

[15] G. D. Watkins and J. W. Corbett, Phys. Rev. **138**, A543 (1965).

[16] It is noted that the anisotropy for the bulk is quite different from that for the aligned V_2^{1-}; sharp peaks appear around 5.0 mrad along the p_y ([011]) and p_x ([$01\bar{1}$]) directions, whereas a deep valley around 5.3 mrad along the [010] direction (*see* Ref. [7]).

[17] L. J. Lantto, Phys. Rev. B **36**, 5160 (1987).

[18] D. R. Hamann, Phys. Rev. B **40**, 2980 (1989); L. Kleinman and D. M. Bylander, Phys. Rev. Lett. **48**, 1425 (1982).

[19] The local potential used in this work is the repulsive Coulomb potential constructed from the effective point charge ($Z_{\text{eff}} = 4$). Even when this potential is replaced by that constructed from the nuclear point and frozen core electron charges, annihilation rates are estimated from the present calculations to vary by less than 1%.

[20] A. Baldereschi, Phys. Rev. B **7**, 5212 (1973).

[21] The calculation with a single sampling (Γ) point gives the FWHMs of the 2D-ACAR cross sections varied by less than 0.02 mrad from the present result.

[22] R. Car and M. Parrinello, Phys. Rev. Lett. **55**, 2471 (1985).

[23] M. C. Payne, M. P. Teter, D. C. Allan, T. A. Arias, and J. D. Joannopoulos, Rev. Mod. Phys. **64**, 1045 (1992).

[24] A. Oshiyama, M. Saito, and O. Sugino, Appl. Surf. Sci. **85**, 239 (1995).